Progress In Electromagnetics Research Letters, Vol. 101, 71–78, 2021

Design of Polarization Insensitive Frequency Selective Surface for Electromagnetic Shielding Application

Surya Durga Padmaja Bikkuri* and S NagaKishore Bhavanam

Abstract—In this paper, a low profile Frequency Selective Surface is presented, for obtaining electromagnetic shielding in four distinct frequency regions. The designed structure consists of three rectangular strips Resonators, Jerusalem cross in the top side and diagonal metallic strips on bottom side of the dielectric. The proposed structure provides electromagnetic shielding at 9.9 GHz, 12.3 GHz, 13.5 GHz, and 16.4 GHz frequency regions. Besides these frequency regions, we also obtain five transparent windows suitable for telemetry application. The prototype of the proposed structure is fabricated. It is observed that the measured results are nearly similar to simulated results because of minor fabrication errors. Furthermore, the proposed low profile structure can be deployed for applications like radome, spatial filters, antenna reflectors, and RCS reductions.

1. INTRODUCTION

Frequency Selective surfaces (FSSs) are formed by periodic arrangements of identical resonant elements in 2D and 3D lattices. These resonant elements, patches, or apertures can allow or restrict the wave propagation in specific frequency bands [1–4]. In several space missions, a sub-reflector made of an FSS was an inevitable part of the antenna unit. For designing a multifunctional antenna unit, a complex multiband FSS structure has also been reported in several literatures [5]. Besides this, FSS became a strong alternative for designing a radome structure. By the help of the frequency filtering property, FSS radome is transparent to the working frequency and is opaque to the frequency out of the frequency band [6, 7]. This spatial filtering property of FSS is also useful for enhancing the gain of the antenna [8, 9] and steering the beam in a particular direction [10]. Notably, for electromagnetic shielding applications, FSS based band stop filter effectively reduces electromagnetic interference [11–13]. Traditionally metallic enclosures are used to provide electromagnetic shielding for electronic circuitry. The main drawback of metallic enclosures is that they block all the frequencies uniformly [14]. The solution to this problem is effectively designing an FSS structure that can be an opaque enclosure to specific frequencies and transparent to others. Transparent window can be used for the telemetry application.

In literature, various geometries of FSS unit cells have been reported for electromagnetic shielding application. A 3D multilayer FSS based structure is reported in [15], where a single band response is observed. Similarly, an ultrawide stopband multilayer FSS with capacitive loading [16] and a three layered FSS dodecagon-shaped unit cell [17] are also reported. However, the lateral dimension and 3D geometry of the structure make them bulky to incorporate in a compact environment. Similarly, a 2.5D FSS based structure using via is also reported [18] for providing band stop characteristics. The structure provides shielding at two bands, but non-planar geometry is not suitable for electromagnetic shielding in a compact environment. Hence, there is a need to design planar and low profile structures for certain applications. Planar multilayer structures are also proposed to achieve higher-order frequency

Received 15 September 2021, Accepted 1 December 2021, Scheduled 6 December 2021
* Corresponding author: Surya Durga Padmaja Bikkuri (padmaja1128@gmail.com).
The authors are with the Department of Electronics and Communication Engineering, Acharya Nagarjuna University, Guntur, Andhra Pradesh, India.

selective characteristics [19, 20] for overcoming the issues of compactness. Even though there is a reduction in lateral dimension, stacking of the layers results in difficulties of misalignment in the fabrication process. To overcome the issue of misalignment, in [21, 22], a single layer FSS is used for EM shielding for wideband operation. However, for shielding telemetry devices, instead of wideband shielding, multiband EM shielding is more desired. Thus, multiband FSS structures gain popularity over single band structures. A dual-band solution is reported in [23] for shielding in ISM and UMII bands. Similarly, a quad-band high profile structure FSS structure is reported in [24] for reducing electromagnetic interferences. However, the passband characteristics of the aforementioned works are not rigorously evaluated.

In this paper, to meet the research gap, a thin quadband FSS structure for electromagnetic shielding application with intermediate passbands is reported. The proposed structure provides shielding at 9.9 GHz, 12.3 GHz, 13.5 GHz, and 16.4 GHz frequency bands, respectively. Moreover, we obtain five transparent windows between the shielded regions suitable for communication purpose. Furthermore, to understand the practicability and robustness of the proposed structure, the performance of FSS at different polarizations for both normal and oblique incidence is analyzed. We observe a stable performance up to 40° for both horizontal and vertical polarizations. For the validation of the simulated result, the structure is fabricated, and measurement is carried out. A good agreement is observed between the measured and simulated results, which confirms the practicability of the structure.

2. DESIGN METHODOLOGY

The proposed multiband FSS structure consists of a Jerusalem cross structure, a rectangular strip ring resonator, and a diagonal cross structure. A schematic diagram of the top and bottom planes of the proposed FSS is depicted in Figs. 1(a) and (b), respectively. The structure is fabricated on both sides of an FR-4 substrate with a thickness of 0.8 mm, permittivity of 4.4, and loss tangent of 0.02. The unit cell of the proposed structure is composed of a periodic arrangement of rectangular strips of length l_1. Each strip differs in length by a dimension of Δl_1. Along with this periodic arrangement of rectangular strips, a Jerusalem cross is also inserted in the center of the top layer. In the bottom layer, a pair of metallic strips is arranged diagonally. The schematic diagram of the unit cell is shown in Figs. 1(a) and (b). The numerically optimized dimensions of the proposed structure are $s = 10$ mm, $l_1 = 8$ mm, $\Delta l_1 = 2$ mm, and $l_2 = 4$ mm. To analyze the electromagnetic behavior of the structure, the transmission and reflection coefficients are plotted in Fig. 1(c). It is observed that at 9.9 GHz, 12.3 GHz, 13.5 GHz, and 16.4 GHz, there is no or negligible transmission.

The amount of electromagnetic shielding exhibited by the proposed surface is measured in terms

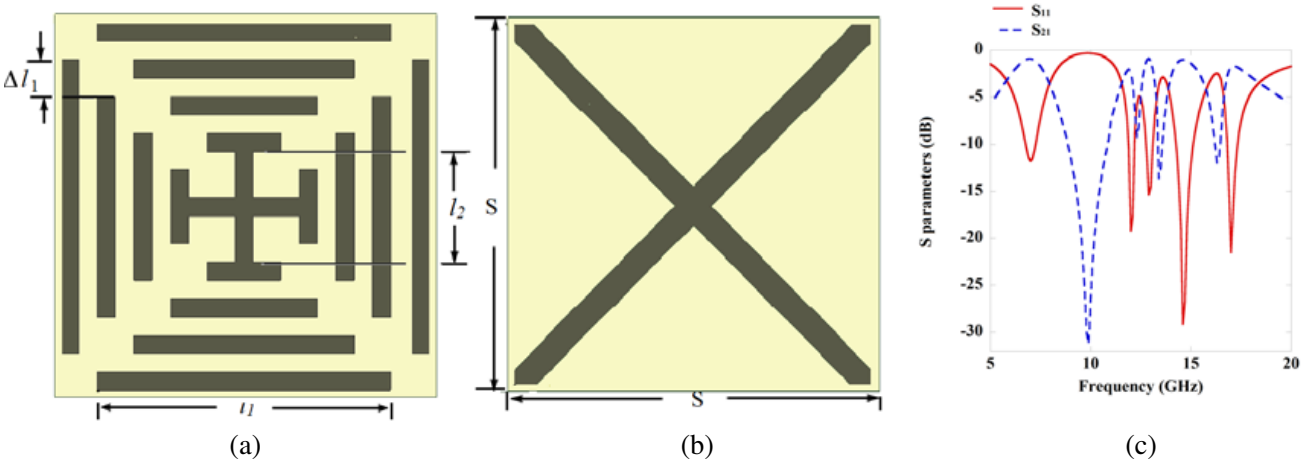

(a) (b) (c)

Figure 1. Proposed unit cell. (a) Schematic of the top layer. (b) Schematic of the bottom layer. (c) S parameter plot of final structure.

of shielding effectiveness. SE shielding effectiveness is expressed as:

$$SE_{\mathrm{dB}} = -20 \log \frac{E_t}{E_i} \tag{1}$$

where E_t and E_i represent the transmitted and incident electric field.

It should be noted from the above equation that SE can also be expressed as the reciprocal of transmission coefficient s_{21}.

To get a clear understanding, electromagnetic behavior of each resonator structure is designed in a step by step manner. It is well known that to achieve multiple stopband characteristic, we need to incorporate multiple resonating structures. Initially, a Jerusalem cross is designed as exhibited in Fig. 2(a). To understand the electromagnetic behavior of the structure, the S parameter response is also analyzed and shown in Fig. 2(a). It is observed from this figure that the structure resonates at the 15.3 GHz frequency region, and a narrow band stop region is observed. In the next stage, we design a triple rectangular strip resonating structure as depicted in the inset of Fig. 2(b). From the S parameter response of this structure (shown in Fig. 2(b)), it is evident that the structure provides stopband frequencies at 11 GHz and 16 GHz. In the later stage, we analyze a diagonal strip structure and monitor its impedance profile. The structure and its impedance response are shown in Fig. 2(c). It is noticed that these diagonal strips offer a significant reactance and negligible resistance throughout the resonating frequencies. The negligible resistance indicates low loss behavior of the structure, whereas the reactance part would provide significant shifting in the resonating frequency of the structure. Finally, we cascaded the structure of Figs. 2(a) and 2(b) in the top layer of the substrate and incorporate the diagonal strip at the bottom side, resulting in four stopbands at 9.9 GHz, 12.3 GHz, 13.5 GHz, and 16.4 GHz frequency with intermediate passband as in Fig. 1(c).

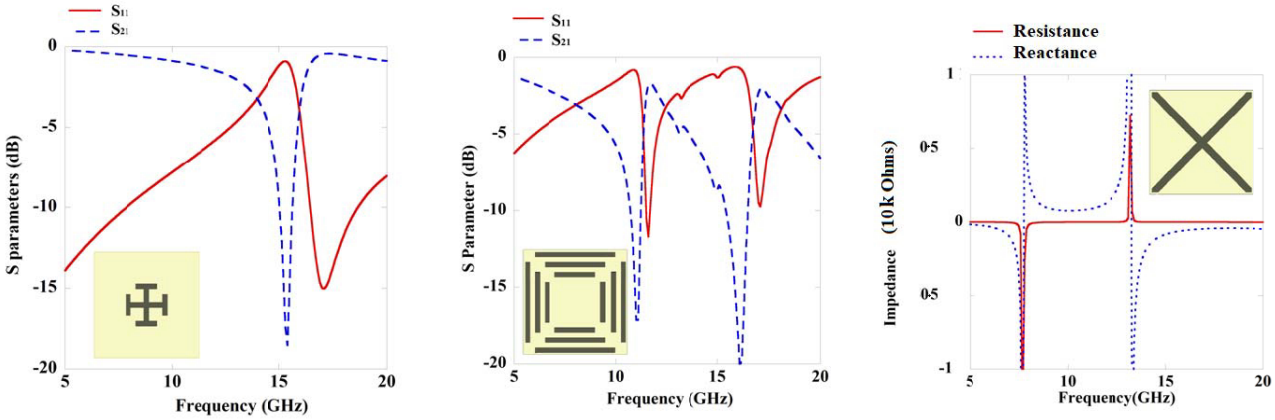

Figure 2. S parameter of (a) Jerusalem cross, (b) triple rectangular strips and (c) impedance plot of diagonal shaped structure. Inset: schematics of the unit cell structure.

To understand electromagnetic behavior, we closely monitor electric field and surface current distribution of each resonator. The magnitude of electric field inside the dielectric layer and the surface currents along the metallic plane are exhibited in Fig. 3(a). For resonator I it is observed that the surface current distributes along the vertical strip at the resonating frequency for TE polarization of incident wave. These vertical strips act as an open ended transmission line. Thus at the open end electric fields are more intense. The surface current in the vertical strip indicates inductive behavior of the structure, and the intensity of electric fields indicates the capacitance behavior of the structure. Similarly, we plot electric field and current distribution of resonator II. From Figs. 3(b) and (c) it is evident that at the lower frequency region the outer strips are more dominant where as for higher frequency inner strips are dominant. This phenomenon is observed in both electric field and surface current distribution. Moreover in the case of electric field, at lower frequency, charges are accumulated at the edge of outer strip and middle strip.

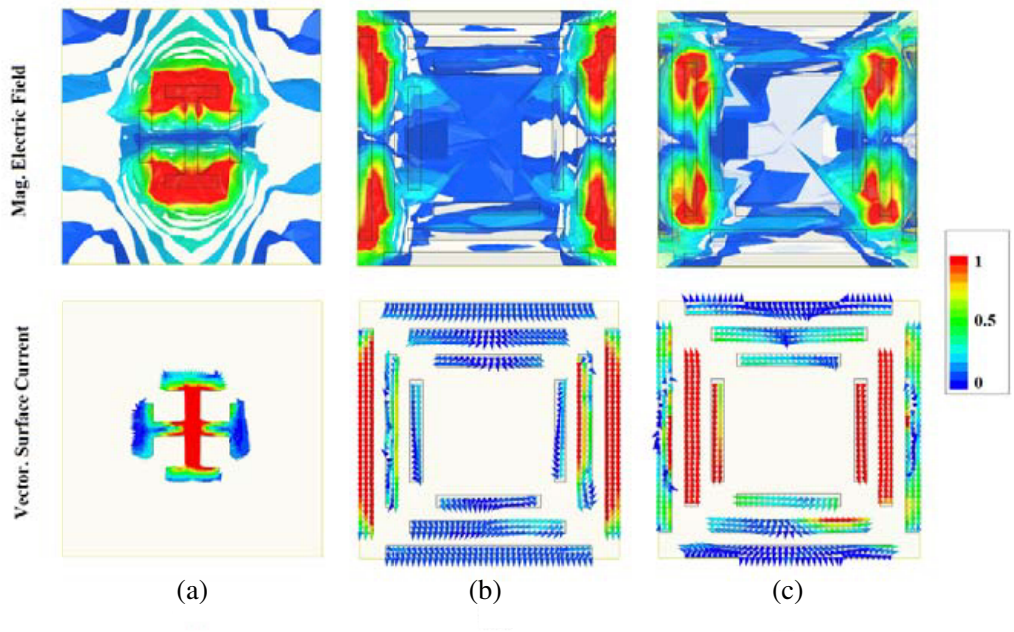

Figure 3. Electric field and surface current, (a) resonator I (15.4 GHz), (b) resonator II (11.3 GHz), (c) resonator II (14.4 GHz).

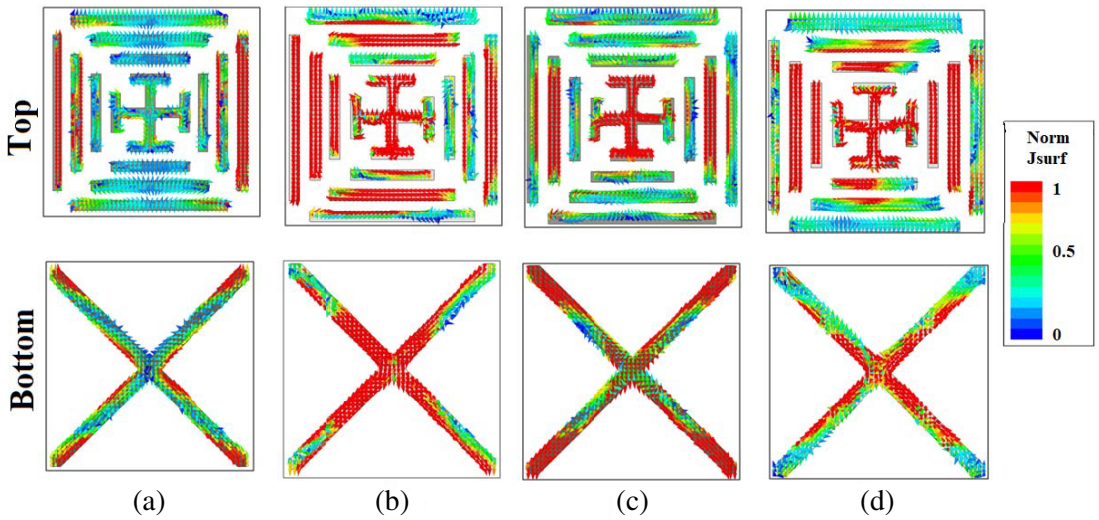

Figure 4. Surface current distribution at (a) 9.9 GHz, (b) 12.3 GHz, (c) 13.5 GHz and (d) 16.4 GHz.

For the higher frequency, the charges accumulated in open edge end of the middle and inner strips. Both of the resonant structures provide filtering characteristics which can be defined by the inductance and capacitance behaviors of the surface. Further to make the structure more compact by incorporating these two resonating structures, one can achieve multi-stopband behavior.

To understand the behavior of the proposed FSS structure, it is required to analyze the surface current distribution at all the four frequency regions for top and bottom layers. The surface current distribution at 9.9 GHz on both sides of the dielectric is shown in Fig. 4(a). From the distribution, it is evident that there are more currents in the rectangular strip of higher dimensions. Similarly, Fig. 4(b) represents the surface current distribution at 12.3 GHz frequency. Observing the current distribution behavior of the FSS, it can be concluded that inter-element capacitance effects exist between these rectangular strips. Because of these capacitance effects, even at a particular frequency of resonance of

that rectangular strip, its nearest neighbour also gets some currents through. It happens the same with Fig. 4(c) and Fig. 4(d), where the structure resonates at 13.5 GHz and 16.4 GHz.

For the validation of simulated results, the proposed prototype is fabricated, and measurement is carried out in an anechoic chamber. An array of a fabricated prototype is shown in Fig. 5(a). Measurement setup comprises two horns and a vector network analyzer (VNA) to record the reflection coefficients of the fabricated structure as shown in Fig. 5(b). The measured results are shown in Fig. 5(b). Multiple measurements were performed to check the uncertainty in the measured results. It is observed that the measured results are in good agreement with the simulated ones. The slight variation in measured results is due to the fabrication imperfections, finite size of FSS, and possible errors in the measurement setup. These variations can be reduced if the size of the FSS is larger.

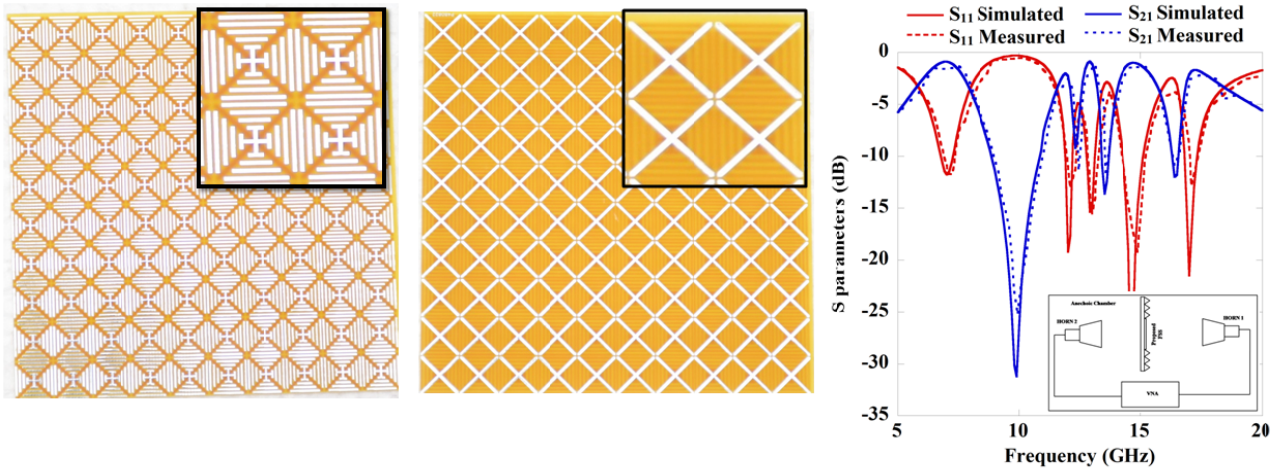

Figure 5. (a) Fabricated FSS prototype (top and back planes). (b) Simulated and measured results of proposed FSS with inset: schematic of testing setup.

To understand the state-of-the-art scenario, a comparison between the other reported FSS structures and proposed work is listed in Table 1. It is observed that the proposed structure has very low profile and provides quad band electromagnetic shielding. Thus, the proposed structure is an attractive choice compared to other reported structures.

Table 1. A comparative analysis of present work with previous reported works.

Ref.	No of Layers	No of Frequency bands	Operating Frequencies	Thickness (mm)
[25]	1	1	10.4 GHz for TE and 14.4 GHz for TM	1.6
[20]	3	1	10.5 GHz	0.4
[22]	1	2	2.55 GHz and 5.7 GHz	1.6
[23]	1	4	0.8 GHz, 0.9 GHz, 1.8 GHz and 1.9 GHz	4
Proposed	1	4	9.9, 12.3, 13.5 and 16.4 GHz	0.8

For the Electromagnetic Shielding application, stable performance of the proposed FSS structure for different polarizations and incident angles is desired. Hence, Floquet port analysis is carried out for different angles of wave incidence for TE and TM polarizations. Due to the geometry of the structure,

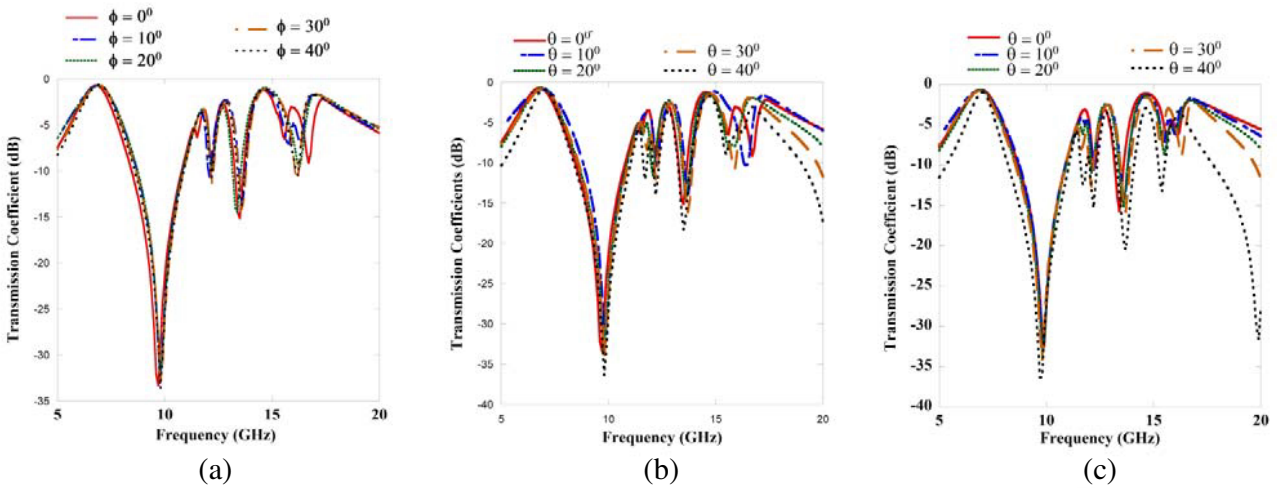

Figure 6. Transmission coefficients of the structure (a) for different polarization, (b) for different angles of incidence in TE polarization, (c) for different angles of incidence in TM polarization.

a slight variation in the reflection coefficients is noticed, which is expected. Still, the structure could maintain angle insensitive behavior up to 40° for both TE and TM polarizations, as shown in Figs. 6(b) and (c). Similarly, reflection coefficients are computed to verify the polarization sensitivity of the structure at different angles of polarization. By observing the plots in Fig. 6(a), the structure response remained polarization insensitive up to 40°.

Therefore, it is evident that the proposed structure exhibited electromagnetic shielding being polarization and incident angle insensitive.

3. CONCLUSIONS

In this paper, a thin quad-band FSS capable of multiband shielding is reported. For achieving multiband shielding, the behaviors of individual resonating structures on the top and bottom layers play a significant role. In addition to this stopband feature, the FSS structure provides five transmission windows that are applicable to the telemetry application. This particular behavior of the structure is verified by fabricating the prototype. From the analysis of simulated and measured results in the microwave region, the proposed FSS is more suitable for shielding the electromagnetic wave in four frequency regions. Due to compact geometry, the structure can be more suitable in applications like radome, electromagnetic shielding, antenna reflector, etc.

REFERENCES

1. Chen, H. Y. and Y. Tao, "Bandwidth enhancement of a U-slot patch antenna using dual-band frequency-selective surface with double rectangular ring elements," *Microwave and Optical Technology Letters*, Vol. 53, No. 7, 1547–1553, 2011.
2. Ghosh, S. and K. V. Srivastava, "Broadband polarization-insensitive tunable frequency selective surface for wideband shielding," *IEEE Transactions on Electromagnetic Compatibility*, Vol. 60, No. 1, 166–172, 2017.
3. Li, J., Q. Zeng, R. Liu, and T. A. Denidni, "A compact dual-band beam-sweeping antenna based on active frequency selective surfaces," *IEEE Transactions on Antennas and Propagation*, Vol. 65, No. 4, 1542–1549, 2017.
4. Sen, G., T. Mandal, S. Majumdar, S. Mahato, S. Mondal, and P. P. Sarkar, "Design of a wide band Frequency Selective Surface (FSS) for multiband operation of reflector antenna," *5th International Conference on Computers and Devices for Communication (CODEC)*, 1–3, December 2012.

5. Romeu, J. and Y. R. Samii, "Fractal FSS: A novel dual-band frequency selective surface," *IEEE Transactions on Antennas and Propagation*, Vol. 48, No. 7, 1097–1105, 2000.
6. Liu, N., X. Sheng, C. Zhang, and D. Guo, "Design of frequency selective surface structure with high angular stability for radome application," *IEEE Antennas and Wireless Propagation Letters*, Vol. 17, No. 1, 138–141, 2017.
7. Jin, C., Q. Lv, B. Zhang, J. Liu, S. An, Z. S. He, and Z. Shen, "Ultra-wide-angle bandpass frequency selective surface," *IEEE Transactions on Antennas and Propagation*, Vol. 69, No. 9, 5673–5681, 2021.
8. Kundu, S., "A compact uniplanar ultra-wideband frequency selective surface for antenna gain improvement and ground penetrating radar application," *International Journal of RF and Microwave Computer-Aided Engineering*, Vol. 30, No. 10, e22363, 2020.
9. Bhattacharya, A., B. Dasgupta, and R. Jyoti, "Design and analysis of ultrathin X-band frequency selective surface structure for gain enhancement of hybrid antenna," *International Journal of RF and Microwave Computer-Aided Engineering*, Vol. 31, No. 2, e22505, 2021.
10. Das, P., K. Mandal, and A. Lalbakhsh, "Single-layer polarization-insensitive frequency selective surface for beam reconfigurability of monopole antennas," *Journal of Electromagnetic Waves and Applications*, Vol. 34, No. 1, 86–102, 2020.
11. Sivasamy, R., M. Kanagasabai, S. Baisakhiya, R. Natarajan, J. K. Pakkathillam, and P. S. Kumar, "A novel shield for GSM 1800 MHz band using frequency selective surface," *Progress In Electromagnetics Research Letters*, Vol. 38, 193–199, 2013.
12. Yu, Z. and C. Wang, "Bandpass frequency selective surface based on square waveguide structure using 3D printing technology," *Progress In Electromagnetics Research M*, Vol. 99, 165–175, 2021.
13. Bilal, M., R. Saleem, Q. H. Abbasi, B. Kasi, M. F. Shafique, "Miniaturized and Flexible FSS-based EM shields for conformal applications," *IEEE Transactions on Electromagnetic Compatibility*, Vol. 62, No. 5, 1703–1710, 2020.
14. Ghosh, J. and D. Mitra, "Restoration of antenna performance in the vicinity of metallic cylinder in implantable scenario," *IET Microwaves, Antennas & Propagation*, Vol. 14, No. 12, 1440–1445, 2020.
15. Lee, I. G. and I. P. Hong, "3D frequency selective surface for stable angle of incidence," *Electronics Letters*, Vol. 50, No. 6, 423–424, 2014.
16. Zheng, G., C. Zhong, L. Tang, P. Luo, and Y. Wang, "Study on ultra-wide stopband miniaturized multilayer frequency selective surface with capacitive loading," *Progress In Electromagnetics Research Letters*, Vol. 94, 117–123, 2020.
17. Shaik, V. and K. Shambavi, "Design of dodecagon unit cell shape based three layered frequency selective surfaces for X band reflection," *Progress In Electromagnetics Research M*, Vol. 75, 103–111, 2018.
18. Yin, W., H. Zhang, T. Zhong, and X. Min, "A novel compact dual-band frequency selective surface for GSM shielding by utilizing a 2.5-dimensional structure," *IEEE Transactions on Electromagnetic Compatibility*, Vol. 60, No. 6, 2057–2060, 2018.
19. Fallah, M., A. Ghayekhloo, and A. Abdolali, "Design of frequency selective band stop shield using analytical method," *Journal of Microwaves, Optoelectronics and Electromagnetic Applications*, Vol. 14, No. 2, 217–228, 2015.
20. Shaik, V. and K. Shambavi, "An ultra-thin non-resonant class of frequency selective surface for X band applications," *Progress In Electromagnetics Research M*, Vol. 96, 9–20, 2020.
21. Syed, I. S., Y. Ranga, L. Matekovits, K. P. Esselle, and S. G. Hay, "A single-layer frequency-selective surface for ultrawideband electromagnetic shielding," *IEEE Transactions on Electromagnetic Compatibility*, Vol. 56, No. 6, 1404–1411, 2014.
22. Da Silva Segundo, F. C. G. and A. L. P. S. Campos, "Compact frequency selective surface with dual band response for WLAN applications," *Microwave and Optical Technology Letters*, Vol. 57, No. 2, 265–268, 2015.

23. Sohail, S. I., "Wi-Fi transmission and multi-band shielding using single-layer frequency selective surface," *IEEE International Symposium on Antennas and Propagation (APSURSI)*, 963–964, June 2016.
24. Paul, G. S., K. Mandal, and A. Lalbakhsh, "Single-layer ultra-wide stop-band frequency selective surface using interconnected square rings," *AEU-International Journal of Electronics and Communications*, Vol. 132, 153630, 2021.
25. Abbasi, S., J. Nourinia, C. Ghobadi, M. Karamirad, and B. Mohammadi, "A sub-wavelength polarization sensitive band-stop FSS with wide angular response for X-and Ku-bands," *AEU-International Journal of Electronics and Communications*, Vol. 89, 85–91, 2018.